İSTANBUL UNIVERSITY CERRAHPAŞA

ORIGINAL ARTICLE
Electrica 2025; 25: 1-10

Two-Cascade Modal Filters Based on Modified Microstrip Lines with Grounded Conductors at the Ends

Indira Y. Sagiyeva, Talgat R. Gazizov, Yevgeniy S. Zhechev

Tomsk State University of Control Systems and Radioelectronics, Tomsk, Russian Federation

Cite this article as: I. Y. Sagiyeva, T. R. Gazizov and Y. S. Zhechev, "Two-cascade modal filters based on modified microstrip lines with grounded conductors at the ends," *Electrica*, 25, 0149, 2025. doi: 10.5152/electrica.2025.24149.

WHAT IS ALREADY KNOWN ON THIS TOPIC?

- *This study builds upon prior research concerning microstrip line (MSL)-based modal filters (MFs) for mitigating ultrashort pulse (USP) interference. This demonstrated the efficacy of a one-cascade MF, comprising an MSL with two side conductors grounded at both ends, in decomposing incident USPs into two lower-amplitude pulses. This conclusion was substantiated by both quasi-static modeling using TALGAT software (TUSUR. EMC) and experimental validation employing vector network analyzers (VNAs) ZVA 40 and P4226, with a high degree of concordance observed between the modeled and measured data. The observed pulse amplitude reduction suggests the MF's potential for transient protection.*

WHAT THIS STUDY ADDS ON THIS TOPIC?

- *The current research extends the previous one by introducing novel two-cascade MF*

Corresponding author:
Indira Y. Sagiyeva,

E-mail:
indira_sagieva@mail.ru

Received: October 30, 2024
Revision requested: November 12, 2024
Last revision received: January 14, 2025
Accepted: January 19, 2025
Publication Date: February 19, 2025

DOI: 10.5152/electrica.2025.24149

ABSTRACT

In this paper, two-cascade connections of three modal filters (MFs) were investigated based on modified microstrip lines (MSLs) with conductors grounded at the ends. It is an MSL with grounded conductors: one top, two symmetrical top, and two side conductors. The study included simulations in the TUSUR.EMC (TALGAT) software based on transmission line analysis and experimental validation using a P4M-18 MICRAN vector network analyzer. The results demonstrated that, due to a two-cascade connection, all three MFs can attenuate the ultrashort pulse (USP) impact by four times by decomposing it into four pulses with small amplitudes. By contrast, a one-cascade connection allows for the pulse attenuation by two times by decomposing the USP into two pulses. Meanwhile, the cross-section parameters and total length can be the same for both one-cascade and two-cascade MFs. Thus, modification by cascade connection can cost-effectively improve the protective properties of MFs against USPs.

Index Terms— Modal filter, microstrip line (MSL), time response, ultrashort pulse (USP)

I. INTRODUCTION

Radio-electronic equipment (REE) is actively developed and introduced into various spheres of human activity [1], which aggravates the problem of ensuring electromagnetic compatibility (EMC) [2]. The increase in device power, the upper frequency of the spectrum of useful signals, and the density of printed circuit board (PCB) layout [3, 4] make REE more susceptible to various electromagnetic interference (EMI) [5]. In addition to interference from useful signals, engineers must consider intentional EMI, especially ultrashort pulses (USPs) [6] that can lead to system malfunctions or even complete failure. In this regard, there is a need to develop new devices that protect REE against EMI. One of them is a modal filter (MF) [7-9] which can be based on microstrip lines (MSLs) [10, 11] and its modifications [12]. The growing susceptibility of REE to EMI of different natures urges researchers to develop new modifications of MFs with better characteristics, efficiency, and reliability. One solution is a series cascade connection, which allows attenuating the input USP by a factor of two at the output of each cascade [13]. At the same time, the cross-sectional parameters of MFs and their total length can be the same for one-cascade as well as for two, three, etc. This modification is important because it provides an opportunity to maximize the attenuation of the impacting USP. Meanwhile, the investigations of this solution have just begun. The purpose of this paper is to summarize recently obtained and present new research results of three two-cascade MFs based on modified MFLs with grounded conductors at the ends [14-17].

II. THE STRUCTURES UNDER STUDY

Previously, we proposed three MFs based on modified MSLs and characterized by the presence of one or two additional conductors connected at the ends to the reference conductor. Let us consider them in more detail.

A. Modal Filter with Grounded Conductor on Top

Fig. 1 shows the first cross-section that can be suitable for both one-cascade and two-cascade MFs.

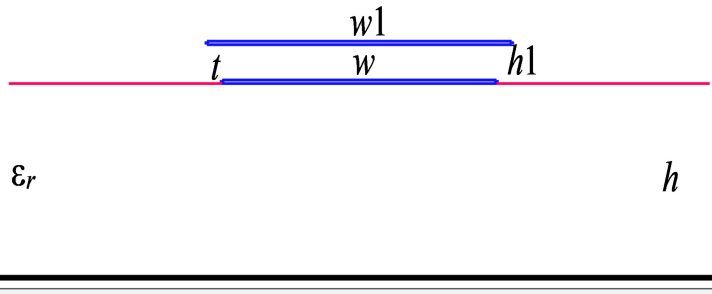

Fig. 1. Modal filter cross-section with grounded conductor on top.

designs that allow considerable increase in USP attenuation performance. A transition from a one-cascade to a two-cascade design, where reference conductors are interconnected at a 1:2 length ratio, was investigated, resulting in the decomposition of incident USPs into four distinct pulses and a two-fold reduction in pulse amplitudes. To assess the performance enhancement, a comparative analysis was performed on one- and two-cascade MFs based on MSLs with two side grounded conductors, using simulation and experimental measurements. The close agreement between simulation and experiments supports the hypothesis that increasing the number of pulse decompositions leads to enhanced USP attenuation..

In this case, a one-cascade MF consists of a reference conductor in the form of a conductive layer, a dielectric substrate on the reference conductor, a signal conductor in the form of a strip on the substrate, and a conductor on top connected at the ends to the reference conductor. The only difference between this MF and a two-cascade MF is that the upper grounded conductor is connected to the reference conductor at a point that divides the line in a 1 : 2 length ratio [14]. This distinction adds only one connection in practice, but in simulation gives the circuit diagram from Fig. 2(B).

B. Modal Filter with Two Symmetrical Grounded Conductors on Top

Fig. 3 shows the second cross-section that is suitable for one- and two-cascade MFs.

In this case, a one-cascade MF has two symmetrical conductors on top rather than one. These conductors are connected at the ends to the reference conductor. A two-cascade MF is characterized by the fact that each upper conductor is connected to a reference conductor at a point that divides the line into two segments in a length ratio of 1 : 2 [15]. The simulated circuit diagrams are shown in Fig. 4.

C. Modal Filter with Two Side-Grounded Conductors

Fig. 5 shows the third cross-section that can be used for one- and two-cascade MFs.

In this case, a one-cascade MF has the two grounded conductors on the sides of the signal conductor instead of the top. In a two-cascade MF, the side conductors are connected to the reference conductor at a point that divides the line into two segments in a length ratio of 1 : 2 [16, 17]. The simulated circuit diagrams are similar to Fig. 4.

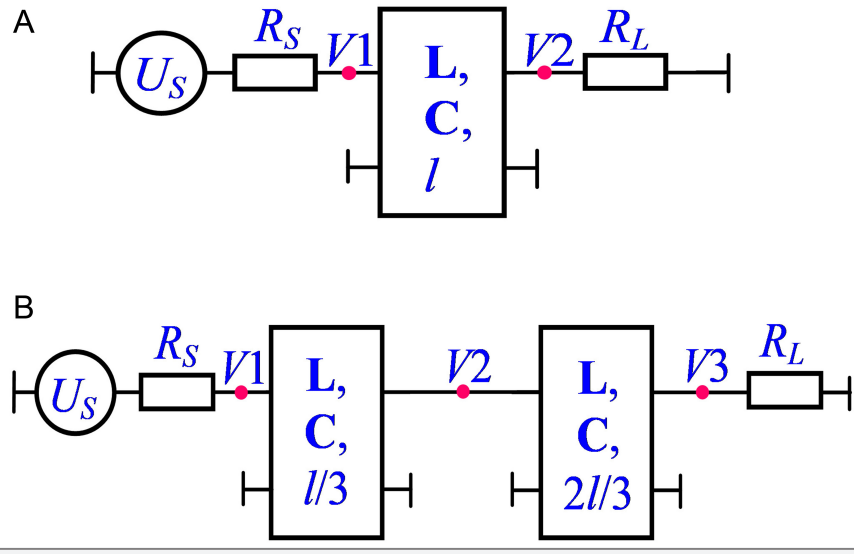

Fig. 2. Circuit diagrams to be simulated: one (A) and two (B) cascade modal filters with grounded conductor on top.

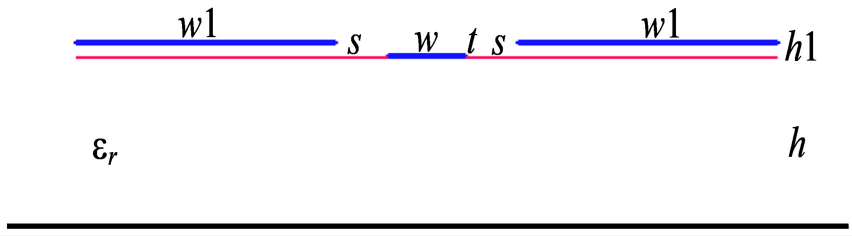

Fig. 3. Modal filter cross-section with two symmetrical grounded conductors on top.

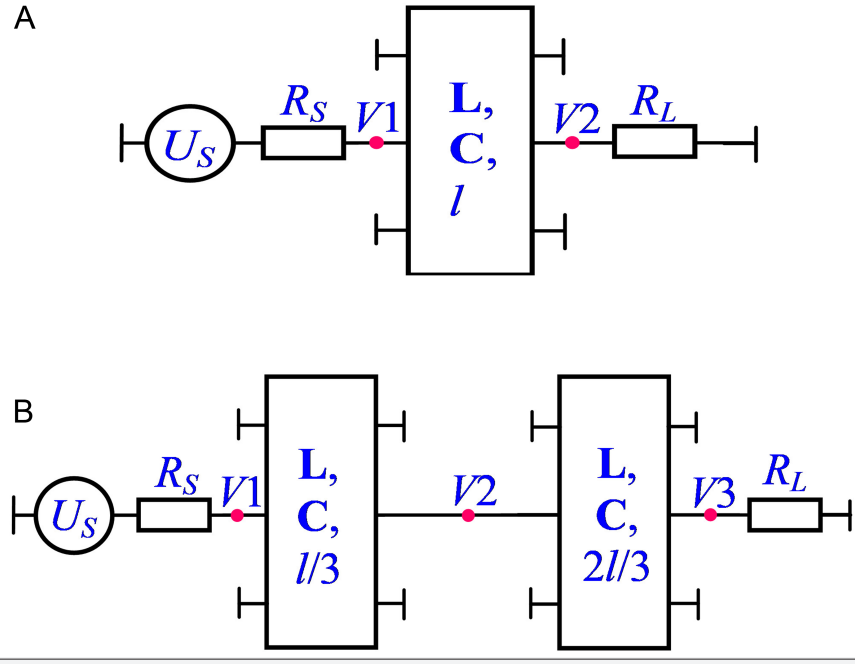

Fig. 4. Circuit diagrams to be simulated: one (A) and two (B) cascade modal filters with two symmetrical grounded conductors on top.

III. SIMULATION RESULTS

In this study, the TUSUR.EMC software, previously known as TALGAT, was used for simulations [18, 19]. This specialized software is designed for quasi-static analysis of multiconductor transmission lines to calculate their time-domain response and frequency characteristics. The simulation process in TUSUR.EMC involves several steps to ensure accurate modeling of the MFs. First, the cross-section of the structure is segmented into small elements to facilitate numerical calculations. (We have set three segments on the conductor thickness (*t*) to achieve an optimal balance between computational efficiency and accuracy.) Then, the numerical method of moments (with a unit step as a basic function and a pulse Dirac function as a test function) is used, which allows highly accurate computation of the per-unit-length electrostatic (**C**) and electromagnetic (**L**) induction coefficients matrices. If the inclusion of losses is required, per-unit-length conductance (*G*) and the resistance (R) matrices are introduced. At last, the software computes the time-domain response of the structure by solving the Heaviside telegraph equations with a trapezoidal USP as an excitation. The pulse with an electromotive force (*E*) with an amplitude of 5 V was applied as the exciting source signal (*Us*) (Figs. 2 and 4). For MFs based on MSLs with one and two grounded conductors on top, the rise, flat top, and fall times were 50 ps each, and with side conductors, they were 30 ps (Fig. 6). This step provides the voltage and current waveforms at different nodes of the structure over time. Also, the frequency-domain characteristics, including the *S*-parameters ($|S_{11}|$ and $|S_{21}|$), are calculated.

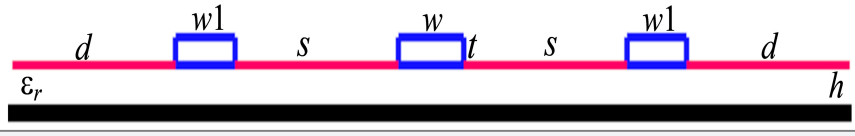

Fig. 5. Modal filter cross-section with two side-grounded conductors.

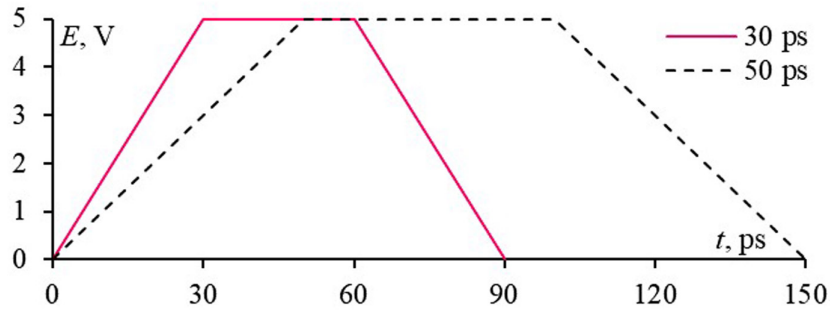

Fig. 6. Electromotive force waveforms of the excitation ultrashort pulse.

Other parameters of the electrical circuit diagrams are as follows: total line length $l = 1$ m, and $R_S = R_L = 50$ Ohm. Losses in conductors and dielectrics were not considered.

A. Modal Filter with Grounded Conductor on Top

General cross-sectional parameters from Fig. 1 are as follows: $t = 18$ μm, $w = 0.9$ mm, $w1 = 1$ mm, $h = 1$ mm, $h1 = 0.2$ mm, and $\varepsilon_r = 4.5$. These parameters determine the matrices of per-unit-length coefficients of the electromagnetic **L** and electrostatic **C** induction of the line. These matrices were computed and presented in Table I.

The square roots of the eigenvalues of the product of these matrices give the per-unit-length delays of the modes propagating in such a line as $\tau1 = 3.42$ ns/m and $\tau2 = 5.84$ ns/m. In the one-cascade MF, the excitation USP is decomposed into two pulses at node *V*2. The interval between them is defined as $l(\tau2 - \tau1)$ and is 2.4 ns with equal amplitudes of 1.2 V (Fig. 7). In the two-cascade MF, the USP is decomposed at node *V*2 into two pulses of smaller amplitudes, with a delay equal to the per-unit-length delay of the corresponding mode multiplied by the length of cascade 1. Each of these pulses is decomposed at node *V*3 into two more pulses, with an additional delay equal to the per-unit-length delay of the corresponding mode multiplied by the length of cascade 2. As a result, the voltage waveform at the line output consists of four pulses with an interval of 0.8 ns between them and equal amplitudes of 0.6 V. This is confirmed by the calculated voltage waveforms at node *V*3 shown in Fig. 7. As a result, the USP attenuation can be increased by a factor of two (compared to the one-cascade MF) if the USP is so short that the decomposed pulses do not overlap.

B. Modal Filters with Two Symmetrical Grounded Conductors on Top

General cross-section parameters from Fig. 3 are as follows: $t = 18$ μm, $w = 0.3$ mm, $w1 = 1$ mm, $h = 1$ mm, $h1 = 0.1$ mm, $s = 0.49$ mm, $\varepsilon_r = 4.5$. The calculated **L** and **C** matrices are presented in Table II.

The mode delays are $\tau1 = 4.23$ ns/m, $\tau2 = 4.37$ ns/m, and $\tau3 = 5.49$ ns/m. However, because of the symmetry of the two upper conductors, the amplitude of the mode 1 pulse is 0, and only the pulses of modes 2 and 3 remain. In this regard, in the one-cascade MF, the excitation USP at node *V*2 is decomposed into two pulses instead of three. The interval between them is 1.12 ns, and the amplitudes are 1.2 V each (Fig. 8). The two-cascade MF works similarly to the one-cascade MF with a grounded conductor on top. As a result, the voltage waveform at the output of node *V*3 is four pulses with 0.37 ns intervals between them and equal amplitudes of 0.6 V. This is confirmed by the calculated voltage waveforms at node *V*3 (Fig. 8). In summary, the attenuation can be increased by a factor of two (compared to the one-cascade MF) of the impacting USP (if it is sufficiently short).

C. Modal Filter with Two Side-Grounded Conductors

General cross-section parameters from Fig. 5 are as follows: $t = 105$ μm, $w = 0.4$ mm, $w1 = 0.365$ mm, $h = 0.18$ mm, $d = 1$ mm, $s = 0.9$ mm, $\varepsilon_r = 4.5$. The calculated **L** and **C** matrices are presented in Table III.

The values of the mode delays are $\tau1 = 5.796$ ns/m, $\tau2 = 5.889$ ns/m, and $\tau3 = 6.089$ ns/m. Additionally, only the pulses of modes 2 and 3 remain because of the symmetry. In this regard, in the one-cascade MF, the USP at node *V*2 is decomposed into only two pulses with an

TABLE I. CALCULATED PER-UNIT-LENGTH MATRICES

L, nH/m	C, pF/m
$\begin{bmatrix} 427.06 & 344.23 \\ 344.23 & 444.63 \end{bmatrix}$	$\begin{bmatrix} 124.43 & -55.35 \\ -55.35 & 69.96 \end{bmatrix}$

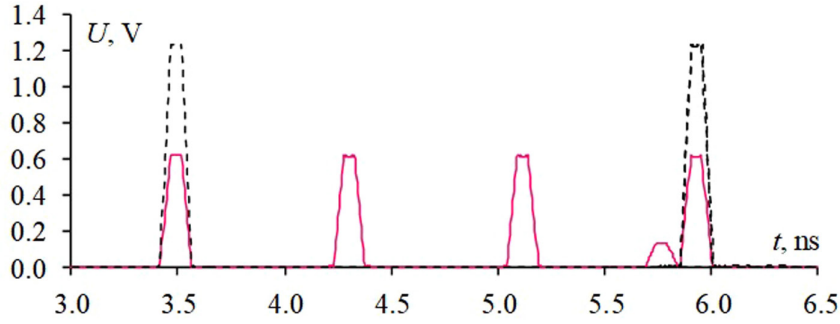

Fig. 7. Voltage waveforms at the ends of one (- -) and two (––) cascade modal filters with grounded conductor at the top.

TABLE II. CALCULATED PER-UNIT-LENGTH MATRICES

L, nH/m			**C, pF/m**		
518.1	235.8	235.8	72.82	–22.06	–22.06
235.8	412.7	147.8	–22.06	60.61	–5.68
235.8	147.7	412.7	–22.06	–5.68	60.61

TABLE III. CALCULATED PER-UNIT-LENGTH MATRICES

L, nH/m			**C, pF/m**		
256.6	11.35	2.777	136.4	–1.423	0.277
11.35	245.2	11.35	–1.423	14.45	–1.423
2.777	11.35	256.6	–0.277	–1.423	136.4

interval of 0.29 ns between them and equal amplitudes of 1.2 V each. The two-cascade MF works similarly to the two-cascade MFs presented above. As a result, the voltage waveform at node *V*3 consists of four pulses with an interval between them of 0.09 ns and equal amplitudes of 0.6 V (Fig. 9). Thus, the attenuation can be increased by a factor of two (compared to the one-cascade MF) of the impacting USP (also sufficiently short).

Additionally, a Bewley's lattice diagram is presented to illustrate the position and direction of each incident, reflected, and transmitted wave (in accordance with each modes) in the transmission line at any given moment in time (Fig. 10). This diagram helps to overcome the challenges associated with tracking multiple successive reflections at various transitions. Its key features are the following: all modes move downward on the diagram as time progresses; the position of any mode at any moment in time can be directly determined from the diagram; and the propagation history of the modes is easy to trace. Fig. 11 shows simulated voltage waveforms at the input and output of the investigated structures.

IV. EXPERIMENTAL STUDIES

The simulation results from Section III were validated by the experiment on the MF prototype with two side-grounded conductors (Fig. 5), which was investigated in detail in ref. [16]. Experimental verification of the developed MFs was performed using a vector network analyzer (VNA) (P4M-18 MICRAN) operating in the 10 MHz–18 GHz frequency range, enabling a direct comparison between the simulation results and the actual measurements (Fig. 12). To prepare for the experiment, MF prototypes were fabricated on a PCB with parameters derived from the simulation stage and were equipped with SMA connectors for easy integration into the measurement setup. Prior to the main measurements, a two-port calibration of the VNA was conducted to minimize errors, and the MFs were connected to the instruments using low-loss RF cables (insertion loss ≤0.5 dB). During testing, the *S*-parameters ($|S_{11}|$, $|S_{21}|$) were recorded over the operating frequency range, confirming the required low-pass characteristics of the filters. Additionally, the obtained frequency-domain data were transformed into the time domain using ADS software, enabling assessment of the USP formation and attenuation

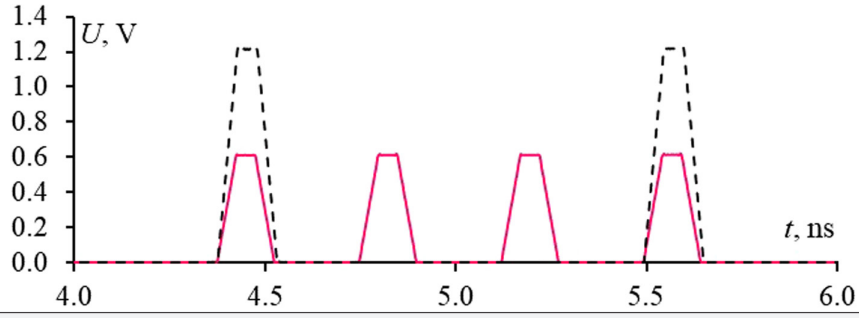

Fig. 8. Voltage waveforms at the ends of one (- -) and two (––) cascade MFs with two symmetrical grounded conductors on top.

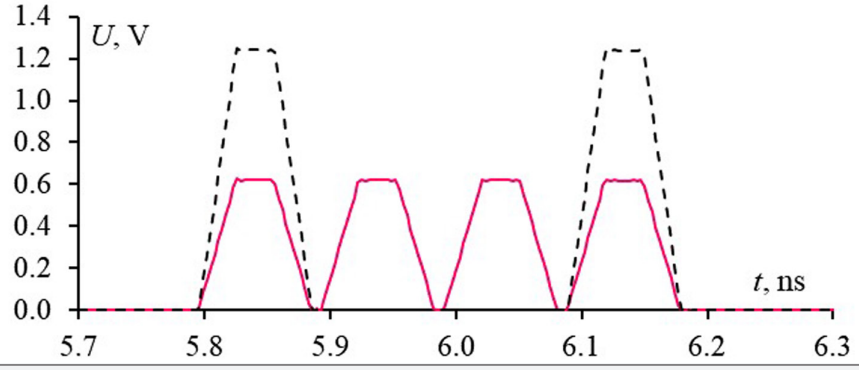

Fig. 9. Voltage waveforms at the ends of one (- -) and two (––) cascade modal filters with two side-grounded conductors.

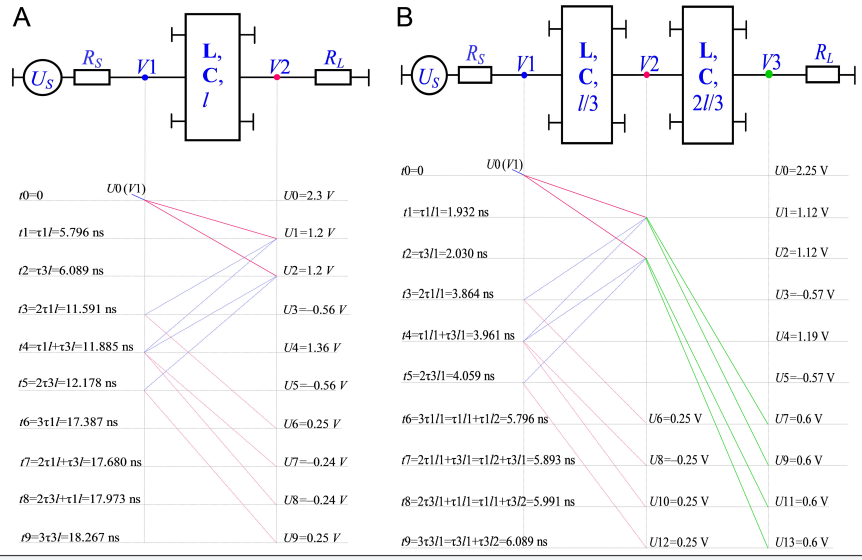

Fig. 10. Bewley's lattice diagrams: one (a) and two (b) cascade modal filters with two side-grounded conductors at nodes *V*1 (––), *V*2 (––), *V*3 (––).

characteristics. The experiment was carried out under controlled laboratory conditions with minimal external EMI.

General parameters are as follows: $t = 70$ μm, $w = 0.45$ mm, $w1 = 0.2$ mm, $h = 0.5$ mm, $d = 1$ mm, $s = 0.45$ mm, $\varepsilon_r = 4$, $tg\delta = 0.03$, $l = 337$ mm. The total dimensions of the PCB were 100 × 100 mm. To reduce its length, the structure was bent into a meander. The coupling between the half-turns was very weak because the distance between them was 10 mm. For the one-cascade MF, the measurements were performed without modifying the prototype, and for the two-cascade MF, the side-grounded conductors of the prototype were connected by vias to the reference conductor in a 1 : 2 length ratio.

Fig. 13 shows the simulation results in the time and frequency domains for one- and two-cascade MFs. It can be seen that in the one-cascade MF, the USP decomposed into two pulses. The amplitude of pulse 1 is higher than that of pulse 2, which may have been caused by the superposition of the edge of pulse 2 on the decay of pulse 1 due to incomplete decomposition. Moreover, it may be due to bigger losses in dielectric fore node 3. In the two-cascade MF, the USP is decomposed into three rather than four pulses because pulses 2 and 3 are superimposed on each other. However, in the two-cascade MF, the pulse amplitudes are smaller than in the one-cascade MF, and the arrival time of pulse 1 is the same in both MFs. Similar results were obtained in the measurements (Fig. 14). Figs. 15 and 16 show the comparison results separately for one- and two-cascade MFs. It can be seen that the pulse delays obtained by measurements and simulations for one- and two-cascade MFs are similar, and the pulse amplitudes from measurements are higher than those from simulations. The maximum differences between measurement and simulation results are observed for two-cascade MFs, namely for pulses 2 and 3. This difference could have arisen due to a number of realities not considered in the simulations. Nevertheless, experimental studies demonstrated the possibility of attenuating the

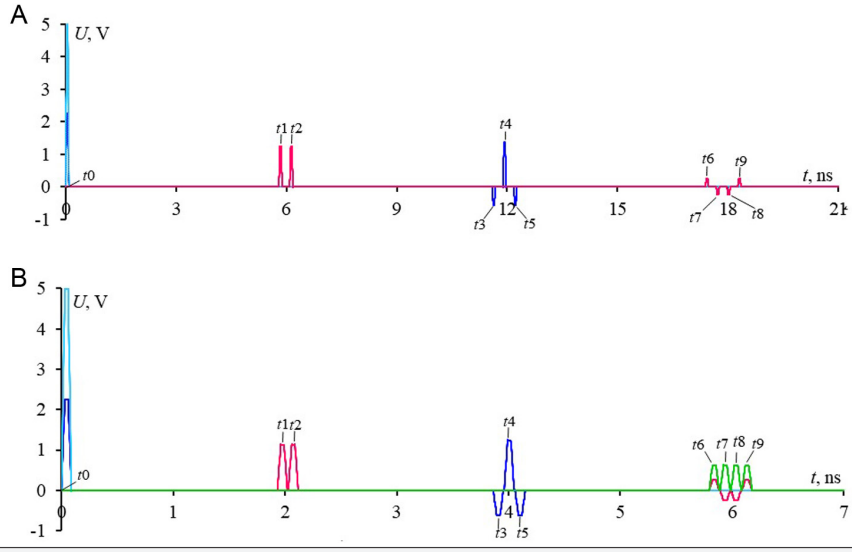

Fig. 11. Voltage waveforms: one (a) and two (b) cascade modal filters with two side-grounded conductors at nodes *V*1 (––), *V*2 (––), *V*3 (––).

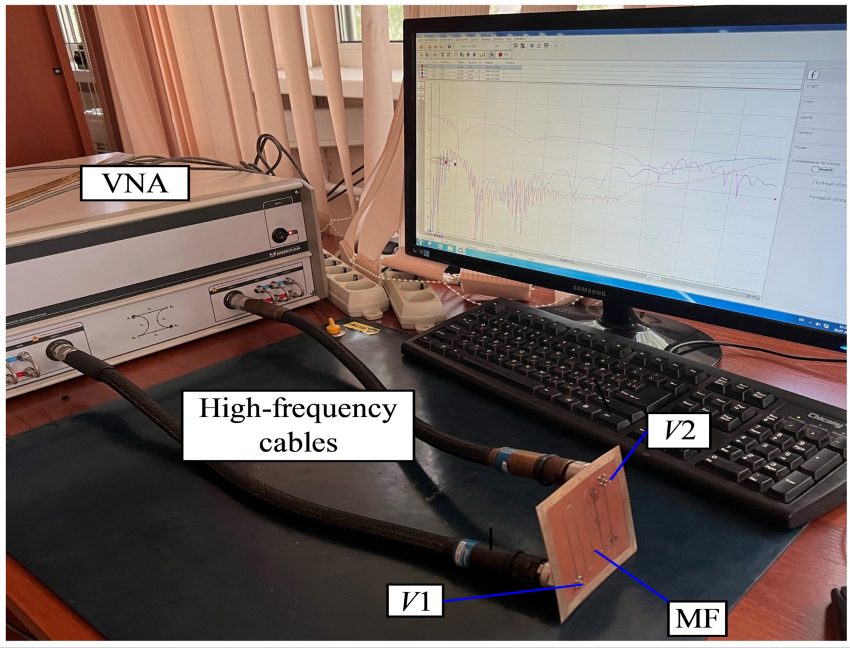

Fig. 12. Experimental setup for analyzing the modal filter frequency characteristics.

impacting USP by two-cascade coupling compared to one-cascade coupling. From the frequency response analysis, it is evident that the studied devices function as low-pass filters of the absorbing or quasi-absorbing type. The passband was measured to be 0.5 GHz for the one-cascade MF and 0.75 GHz for the two-cascade MF. This means more wideband useful signal propagation in two-cascade MF.

V. DISCUSSION

The effectiveness of the proposed two-cascade MF was evaluated by comparing its key characteristics with existing solutions based on modal filtering for EMI suppression. Unlike traditional LPFs (Low-pass filters), which primarily reflect interference signals, the proposed MF leverages modal decomposition to split USPs into multiple lower-amplitude pulses, reducing the risk of equipment damage. Additionally, the cascading configuration enhances the attenuation of interference without increasing the device's physical dimensions. The proposed MF achieves attenuation levels comparable to state-of-the-art solutions. Compared to investigated MFs and meander lines, the two-cascade MF maintains a compact footprint while achieving superior performance in decomposing USPs.

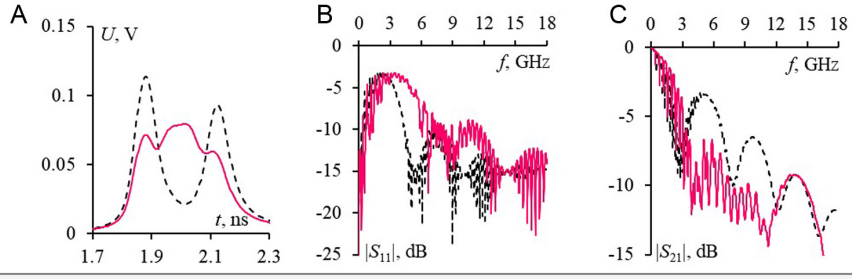

Fig. 13. Simulated voltage waveforms at the one (- -) and two (–-) cascade modal filter output (A) and their $|S_{11}|$ (B) and $|S_{21}|$ (C).

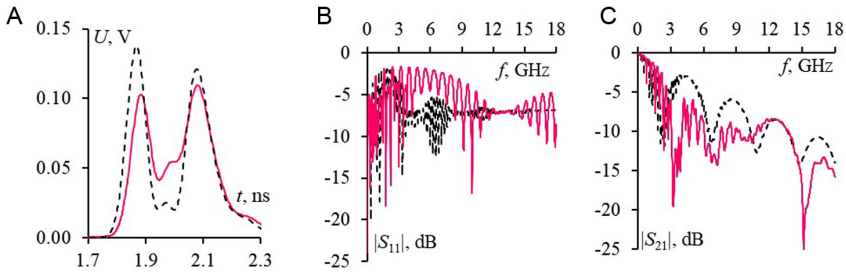

Fig. 14. Measured voltage waveforms at the one (- -) and two (–-) cascade modal filter output (A) and their $|S_{11}|$ (B) and $|S_{21}|$ (C).

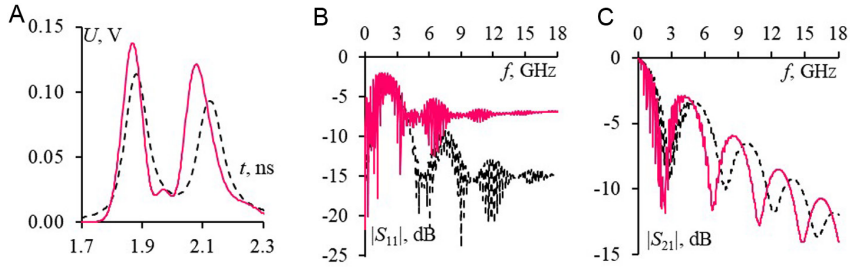

Fig. 15. Voltage waveforms at the one-cascade modal filter output obtained by simulation (- -) and measurement (––) (A) and their $|S_{11}|$ (B) and |S21| (C).

Through cascading, the proposed MF achieves a reduction in pulse amplitude by a factor of four, outperforming traditional single-cascade MFs, which typically achieve only a two-fold reduction. Unlike conventional LPFs, the MF minimizes internal reflections, reducing unwanted interference in systems with complex channel frequency separation. Table IV compares the proposed MF with representative solutions from the literature, focusing on parameters such as compactness and bandwidth. The data confirms that the cascading approach significantly enhances performance metrics, especially in high-frequency applications.

The proposed two-stage MF design offers tangible benefits for protecting critical electronic equipment from USPs in complex electromagnetic environments. Integrating these MFs into PCBs of telecommunications hardware, such as base stations, satellite links, and emerging 5G infrastructure, enhances reliability and stability without adding unnecessary complexity. Military and aerospace sectors also stand to gain by applying this approach in settings like military vehicles, aircraft, and satellites, where deliberate threats in the form of intentional EMI or high-power microwaves can compromise sensitive electronics. Industrial automation and control systems benefit as well, since the MF arrangement provides a shield against pulses generated by switching devices or external sources, thereby sustaining continuous operation. The medical field, reliant on precise imaging and monitoring equipment, can ensure consistent performance and reduce the risk of EMI in hospital environments by adopting these filters. Even the ever-expanding Internet of Things can exploit the compact, two-stage MF design to improve

TABLE IV. PERFORMANCE SUMMARY AND COMPARISONS

	[8]					This Work	
Reference	**The Design I**	**The Design II**	**[20]**	**[21]**	**[22]**	**One-Cascade MF**	**Two-Cascade MF**
Platform	Strip line	Strip line	Microstrip line	Microstrip line	Strip line	Microstrip line	Microstrip line
Board material	FR-4	FR-4	FR-4	FSD1020T	FR-4	FR-4	FR-4
f_c (GHz)	0.069	0.089	1	0.084	1.67	0.5	0.75
Average value of the insertion loss in the pass band (dB)	1.65	1.25	1.1	1.7	1.6	1.7	1.25
Size (mm^2)	125 × 35	125 × 47	110 × 40	18 × 14	200 × 9.3	70 × 70	70 × 70
Length of the structure (mm)	300	300	90	200	200	337	337
Number of decomposed pulses	2	2	2	3	4	2	4

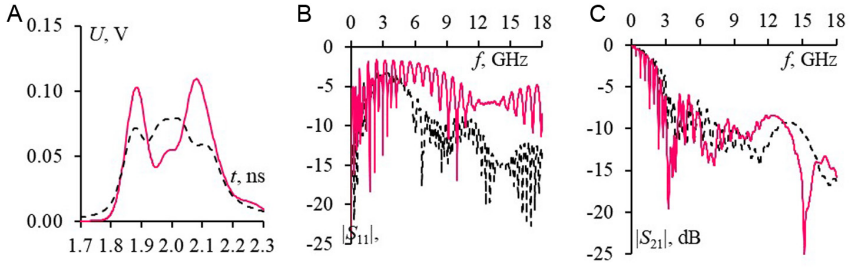

Fig. 16. Voltage waveforms at the two-cascade modal filter output obtained by simulation (- -) and measurement (––) (A) and their $|S_{11}|$ (B) and |S21| (C).

resilience in dense and unpredictable electromagnetic conditions, minimizing external disturbances and enhancing network robustness. In all these applications, the MF structure reinforces protection against electromagnetic threats without incurring substantial cost increments or complicating system designs, making it a versatile and attractive solution for a wide range of modern electronic platforms.

VI. CONCLUSION

Thus, this paper presents a generalized and more detailed study of two-cascade MFs based on three MSLs with grounded conductors at the ends: one on top, two symmetrical on top, and two side conductors. The studies were performed by simulations in the TUSUR. EMC system based on the TL analysis and measurements with VNA R4M-18 MICRAN. As a result, all three modified MSLs previously investigated by the authors can improve MF properties and enhance protection against USPs. Note that cascading allows improving the MFs without additional cost (material and financial).

Availability of Data and Materials: The data that support the findings of this study are available on request from the corresponding author.

Peer-review: Externally peer-reviewed.

Author Contributions: Concept – I.Y.S., T.R.G.; Design – I.Y.S., Y.S.Z.; Supervision – T.R.G.; Funding – I.Y.S., T.R.G., Y.S.Z.; Materials – I.Y.S.; Data Collection and/or Processing – I.Y.S., Y.S.Z.; Analysis and/or Interpretation – T.R.G.; Literature Search – I.Y.S.; Writing – I.Y.S.; Critical Review – T.R.G.

Declaration of Interests: The authors have no conflicts of interest to declare.

Funding: The study was supported by the Ministry of Science and Higher Education of the Russian Federation (Grant no: FEWM-2024-0005).

REFERENCES

1. B. Volochiy, B. Mandziy, and L. Ozirkovskyy, "New features of reliability engineering technology of radioelectronic systems," 2014, *Research Gate*.
2. H. Rozorinov, O. Hres, V. Rusyn, and P. Shpatar, "Environment of electromagnetic compatibility of radio-electronic communication means," *IAPGOS*, vol. 10, no. 1, pp.16–19, 2020. [CrossRef]
3. W. Jillek, and W. K. C. Yung, "Embedded components in printed circuit boards: A processing technology review," *Int. J. Adv. Manuf. Technol.*, vol. 25, no. 3–4, pp. 350–360, 2005. [CrossRef]
4. M. I. Montrose, *Printed Circuit Board Design Techniques for EMC Compliance–A Handbook for Designers, Second Edition*. New York, United States of America: IEEE Institute of Electrical and Electronics Engineers, pp. 1–340.
5. T. Ji, and W. Li, "Simulation of the high power electromagnetic pulse radiation effect on shielded electronic system," *Optoelectronics*, pp.141–151, 2019.
6. M. Polyanskiy, and M. Babzien, "'Ultrashort Pulses,' *in book*," vol. CO_2 *Laser - Optimisation and Application*, 2012.
7. A. T. Gazizov, A. M. Zabolotsky, and T. R. Gazizov, "UWB pulse decomposition in simple printed structures," *IEEE Trans. Electromagn. Compat.*, vol. 58, no. 4, pp. 1136–1142, 2016. [CrossRef]
8. M. A. Samoylichenko, Y. S. Zhechev, V. P. Kosteletskii, and T. R. Gazizov, "Electrical characteristics of a modal filter with a passive conductor in the reference plane cutout," in *IEEE Trans. Electromagn. Compat.*, vol. 63, no. 2, pp. 435–442, 2021. [CrossRef]
9. V. O. Gordeyeva, and A. O. Belousov, "Experimental study of a modal filter based on a round cable structure," *Syst. Control. Commun. Sec.*, vol. 2, pp. 173–192 (in Russian), 2024.
10. L. G. Maloratsky, "Using modified microstrip lines to improve circuit performance," in *High Freq. Electron.*, vol. 10, no. 5, pp. 38–52, 2011.
11. D. Packiaraj, M. Ramesh, A. T. Kalghatgi, and K. J. Vinoy, "Analysis of modified microstrip line and its application," National Conference on Communications, 2012, pp. 1–4. [CrossRef]
12. E. B. Chernikova, A. A. Kvasnikov, A. M. Zabolotsky, and S. P. Kuksenko, "Evaluating the influence of the magnetic permeability of the microstrip modal filter substrate on its frequency characteristics," *J. Phys. Conf. S.*, vol. 1611, no. 1, pp. 1–4, 2020. [CrossRef]
13. A. O. Belousov, "Cascading of three-conductor modal filters based on asymmetric coaxial structures and the microstrip line," *J. Commun. Technol. Electron.*, vol. 68, no. 5, pp. 601–608, 2023. [CrossRef]
14. I. Y. Sagiyeva, T. R. Gazizov, and A. Sekenova, "Patent of Russian Federation No. 2784034," *Two-Step Microstrip Line with a Grounded Conductor on the Top, Protecting against Ultrashort Pulses*, 2022.
15. I. Y. Sagiyeva, T. R. Gazizov, and A. Sekenova, "Patent of Russian Federation No. 2788187," *Two-Segment Microstrip Line with Two Symmetrical Conductors on Top, Protecting against Ultrashort Pulses*, 2023.
16. I. Y. Sagiyeva, and T. R. Gazizov, "Simple modal filter based on microstrip line," *Electrica*, vol. 23, no.3, pp. 516–521, 2023. [CrossRef]
17. I. Y. Sagiyeva, Y. S. Zhechev, Z. M. Kenzhegulova, R. S. Surovtsev, and T. R. Gazizov, "Modal filter based on a microstrip line with two side conductors grounded at both ends," *IEEE Trans. Electromagn. Compat.*, vol. 65, no.5, pp. 1371–1378, 2023. [CrossRef]
18. S. P. Kuksenko, "Preliminary results of a project of the University of TUSUR on designing the distribution network space vehicles: Modeling EMC," *IOP Conf. S. Mater. Sci. Eng.*, vol. 560, no. 012110, pp. 1–7, 2019.
19. A. E. Maksimov, "Use of adaptive cross approximation and block iterative solution of a matrix equations sequence in multivariate analysis of multiconductor transmission lines by the method of moments," *Syst. Control. Commun. Sec.*, vol. 3, pp. 197–226 (in Russian), 2023.
20. R. S. Surovtsev, A. V. Nosov, A. M. Zabolotsky, and T. R. Gazizov, "Possibility of protection against UWB pulses based on a turn of a meander microstrip line," *IEEE Trans. Electromagn. Compat.*, vol. 59, no. 6, pp. 1864–1871, 2017. [CrossRef]
21. K. P. Malygin, A. V. Nosov, and K. P. Malygin, "Experimental confirmation of ultrashort pulse decomposition in folded meander microstrip lines," *IEEE Trans. Electromagn. Compat.*, vol. 65, no.5, pp. 599–605, 2023.
22. Y. S. Zhechev, E. B. Chernikova, and A. M. Zabolotsky, "Reflectionless low-pass filters based on reflection symmetric structure for IEMI suppression," *IEEE Trans. Electromagn. Compat.*, vol. 11, pp. 1–11, 2024. [CrossRef]

Indira Y. Sagiyeva was born in 1992. In 2014, she received a B.Sc. degree from Almaty University of Energy and Communications, Almaty, Kazakhstan, and in 2016 – a M.Sc. degree from Tomsk State University of Control Systems and Radioelectronics (TUSUR), Tomsk, Russia. In 2020, after graduating from TUSUR, she qualified as a teacher-researcher. In 2021, she received a PhD degree in Antennas, Microwave Devices and their Technology. Currently, she works as a senior research fellow at TUSUR. She is the author and co-author of 70 scientific papers.

Talgat R. Gazizov was born in Jalal-Abad, Kyrgyzstan, in 1963. He received the Ph.D. degree in Improvement of Circuit Board Interconnections and the D.Sc. degree in Reduction of Electric Signal Distortions in the Interconnections and Effects of Power Electromagnetic Interference from Tomsk State University of Control Systems and Radioelectronics, Tomsk, Russia, in 1999, and 2010, respectively. He has authored/coauthored more than 524 scientific papers, including 11 books. His research interests include signal integrity problems.

Yevgeniy S. Zhechev was born in Almaty, Kazakhstan, in 1994. He received the B.Sc., M.Sc. and PhD degrees in Infocommunication Technologies and Communication Systems from Tomsk State University of Control Systems and Radioelectronics, Tomsk, Russia, in 2016, 2018, and 2022, respectively. He has over 8 years of experience with electromagnetic compatibility issues. His current research interests include time-domain electromagnetic simulation techniques, electromagnetic compatibility, microwave transmission lines, and protective devices. He has authored or co-authored over 100 refereed publications.